

1 Article

2

Influence of Synoptic-Scale Air Mass Conditions on

3

Seasonal Precipitation Patterns over North Carolina

4 Christopher Zarzar ^{1*} and Jamie Dyer ²5 ¹ Environmental Program, Department of Biology, Wake Forest University, Winston-Salem, North Carolina,
6 USA; zarzarc@wfu.edu7 ² Department of Geosciences, Mississippi State University, Mississippi State, Mississippi, USA;
8 jamie.dyer@msstate.edu

9 * Correspondence: zarzarc@wfu.edu

10

11 **Abstract:** This paper characterizes the influence of synoptic-scale air mass conditions on spatial and
12 temporal patterns of precipitation in North Carolina over a 16-year period (2003–2018). National
13 Center for Environmental Prediction Stage IV multi-sensor precipitation estimates were used to
14 describe seasonal variations in precipitation in the context of prevailing air mass conditions
15 classified using the spatial synoptic classification system. Spatial analyses identified significant
16 clustering of high daily precipitation amounts distributed along the east side of the Appalachian
17 Mountains and along the coastal plains. Significant and heterogeneous clustering was prevalent in
18 summer months and tended to coincide with land cover boundaries and complex terrain. The
19 summer months were dominated by maritime tropical air mass conditions whereas dry moderate
20 air mass conditions prevailed in the winter, spring, and fall. Between the three geographic regions
21 of North Carolina, highest precipitation amounts were received in western North Carolina during
22 the winter and spring, and in eastern North Carolina in the summer and fall. Central North Carolina
23 received the least amount of precipitation; however, there was substantial variability between
24 regions due to prevailing air mass conditions. There was an observed shift toward warmer and more
25 humid air mass conditions in the winter, spring, and fall months throughout the study period (2003–
26 2018), indicating a shift toward air mass conditions conducive to higher daily average rain rates in
27 North Carolina.

28 **Keywords:** precipitation; seasonal; air mass; spatial patterns

29

30

1. Introduction

31 Knowledge of precipitation variability is essential to improving the forecasting and mitigation
32 of hydrological hazards. Rapid population growth and increasing urban density act both to
33 exacerbate human susceptibility to hydrological hazards and increase precipitation sensitivity to
34 anthropogenic modifications to surface land cover conditions and climate change [1]. This is
35 especially true in the Southeast United States which is home to some of the faster growing areas in
36 the United States [2].

37 Precipitation in the southeastern United States has strong seasonal and regional sensitivity due
38 to variations in mid-latitude cyclone frequency [3], tropical cyclones [4], orographic processes [5], sea
39 breeze circulations [6], and local-scale thermodynamic forcing [7]. Analyses of long-term
40 precipitation patterns and trends over the Southeast United States tend to rely on dense rain-gauge
41 networks [8,9], although such data sources often have poor spatial coverage. Passive satellite remote
42 sensing platforms have been used to explore the spatial characteristics of precipitation, especially
43 around large metropolitan areas [10]; however, because precipitation distribution is known to vary
44 with scale [11], studies have more recently used fine temporal and spatial radar-derived precipitation
45 estimates for the analysis of spatio-temporal precipitation patterns at greater detail [12]. Furthermore,
46 radar coverage in the Southeast United States has been shown to reproduce precipitation

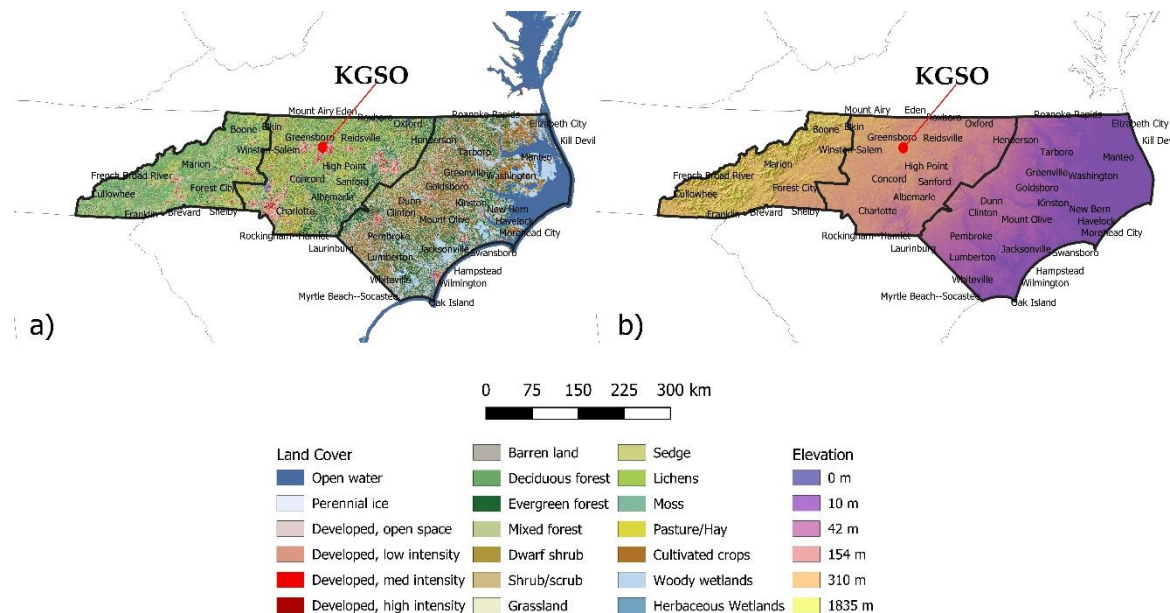
47 observations comparable to surface gauges [13,14]. The advent of radar-based multi-sensor
48 precipitation datasets has further improved the accuracy of radar-based precipitation estimates.
49 These multi-sensor datasets augment radar data with surface rain gauge and satellite precipitation
50 estimates to address the caveats associated with radar estimates, especially over complex terrain.
51 While these types of data and algorithms are becoming more viable for scientific analysis due to
52 longer periods of record, the application of these multi-sensor precipitation data in characterizing
53 long-term precipitation patterns across the Southeast United States has been limited [15,16].

54 Precipitation in the cool season tends to be associated with the passage of mid-latitude cyclones
55 [3], while warm-season precipitation is often linked with local-scale thermodynamic forcing induced
56 by variations in land-cover and soil characteristics [6,17] and tends to occur in the late afternoon and
57 evening [18]. In a long-term study over North Carolina, Sayemuzzaman and Jha [9] noted that the
58 majority of North Carolina rain gauge stations experienced a negative trend in wintertime
59 precipitation and a positive trend in summertime precipitation. These seasonal precipitation trends
60 may indicate a shift from more homogenous synoptically driven precipitation events to more
61 heterogeneous thermodynamically driven precipitation events, which would have important
62 implications on stormwater management, water resource allocation, and agricultural operations.
63 Furthermore, there has been a notable increase in the urban heat island signal across the central
64 portion of North Carolina [19]. The combined effect of increasing summertime precipitation and
65 increasing urban heat island signals points toward more intense and spatially heterogeneous
66 precipitation patterns [20,21]; however, the magnitude of this signal will be dictated by the prevailing
67 synoptic scale air mass. For example, a seasonal shift in days under dry polar (DP) air mass regimes
68 to days under moist tropical (MT) air mass regimes would enhance the thermodynamic forcing of
69 precipitation by increasing the surface energy fluxes [22].

70 The objective of this study is to quantify the spatial and temporal patterns of precipitation
71 across North Carolina, USA in relation to synoptic-scale air mass classification. North Carolina is a
72 unique natural laboratory for studying precipitation because of the distinct geographic features
73 separating three regions across the state, and because of natural variability in annual and seasonal
74 precipitation regimes. The presented analysis uses multi-sensor data from the National Center for
75 Environmental Prediction (NCEP) to define spatial precipitation patterns over a 16-year period (2003–
76 2018). In addition to studying the seasonal spatial variability in precipitation, this paper will place
77 the analysis in the context of prevailing air mass conditions to investigate how variations in synoptic-
78 scale forcing, or lack thereof, influence seasonal precipitation regimes across the study domain. This
79 will be important for the forecasting and mitigation of hydrologic hazards, especially in response to
80 rapid population growth and urbanization across North Carolina.

81 2. Materials and Methods

82 North Carolina offers a unique natural laboratory because it displays a large variety of
83 topographic, soil type, and land use characteristics, including mountainous terrain, dense forests,
84 agricultural lands, metropolitan cities, and low relief coastal regions (Figure 1).



85

86 Figure 1. a) National Land Cover Database (NLCD) 2016 data and b) elevation. Three regions are
 87 delineated from left to right as western North Carolina, central North Carolina, and eastern North
 88 Carolina.

89 The state is comprised of three geologically distinct regions. Western North Carolina (WNC) is
 90 characterized by complex terrain in the Appalachian Mountains covered by a mix of deciduous
 91 forests and boreal conifer forests with thick underbrush, as well as a sparse matrix of urban regions.
 92 The Piedmont region of central North Carolina (CNC) is a dramatic transition in both vegetation and
 93 soil characteristics from the western mountains to the eastern coastal lowlands. CNC transitions from
 94 the WNC deciduous and conifer forests to heavy agricultural and urban landcover, and has the
 95 highest population density and fastest population growth of the three regions leading to an
 96 increasing trend in impervious surfaces [19,23]. The coastal plains in eastern North Carolina (ENC)
 97 are characterized by sparsely populated cities, widespread livestock operations, and hardwood
 98 swamp forests in the eastern coastal lowlands.

99 The current study utilized 16 years (2003-2018) of the NCEP Stage IV multi-sensor precipitation
 100 estimates product [24]. The NCEP Stage IV product is produced by mosaicking twelve National
 101 Weather Service (NWS) River Forecast Center (RFC) hourly Next Generation Weather Radar
 102 (NEXRAD) Stage III/Multi-sensor Precipitation Estimator (MPE) products [25]. The Stage III/MPE
 103 product is a radar-based precipitation dataset that combines ground and space-derived precipitation
 104 estimates and is quality controlled at each RFC. As such, the final Stage IV product produces hourly
 105 and daily best estimate gridded precipitation products projected on the Hydrologic Rainfall Analysis
 106 Project (HRAP) polar stereographic coordinate system centered at 60°N/105°W with a nominal 4 x 4
 107 km grid resolution. Nelson [26] noted concerns using the hourly estimates due to the automated
 108 hourly quality control procedures used at RFCs; therefore, the manually quality controlled daily
 109 NCEP Stage IV gridded binary (GRIB I) product was used in the current study.

110 The spatial synoptic classification (SSC) [22] data from the Greensboro station (KGSO) were used
 111 to identify the prevailing air mass conditions for each day in the dataset. KGSO was selected because
 112 it is a centrally located SSC site in North Carolina and was representative of the prevailing air mass
 113 conditions over all three regions. While air mass extents are generally accepted to be larger than the
 114 state of North Carolina, it was necessary to justify the viability of using a single, centrally located site.
 115 After running a correlation between the Asheville, NC, Greensboro, NC, and Hatteras, NC SSC sites,
 116 the results showed moderate agreement. Furthermore, air mass types along the coast would be less
 117 variable due to higher station humidity level, while the air mass conditions over the mountains
 118 would be highly variable, especially since the air mass is defined by site specific conditions. As a

119 result, a location in the center of the state was identified as the most representative of the general
120 regional air mass conditions.

121 Classification of the different air masses by the SSC developed by Sheridan [22] first identifies
122 baseline conditions at each site by selecting seed days that describe typical meteorological
123 characteristics during each air mass condition including: temperature, dew point depression, mean
124 cloud cover, mean sea level pressure, diurnal temperature range, and diurnal dew point range. With
125 the SSC system, it is possible to classify the prevailing air mass into one of seven categories:
126 transitional (TR), moist tropical (MT), moist moderate (MM), moist polar (MP), dry tropical (DT), dry
127 moderate (DM), and dry polar (DP) (Table 1). For example, many urban heat island studies focus on
128 MT days because this air mass is typically associated with synoptically benign days that experience
129 conditional instability conducive to thermodynamically driven convection [20–22,27]. Additional
130 details on the development of the SSC dataset are provided by Sheridan
131 [<http://sheridan.geog.kent.edu/ssc.html>, 22]. In the current study, we incorporated all classifications
132 to consider the impact of the prevailing air mass on seasonal spatial and temporal precipitation
133 patterns.

134 Table 1. Air mass classification type from the SSC [22].

135

Air Mass	Description
Transitional (TR)	Days with transitioning air mass conditions. Large shifts in pressure, dew point, and wind.
Moist Tropical (MT)	Warm and very humid conditions. Often associated with southerly flow. Typically found in warm sector of mid-latitude cyclones.
Moist Moderate (MM)	Cool and humid conditions. Can form as a modified MP. Can also occur in summer under MT conditions with dense cloud cover.
Moist Polar (MP)	Cool, cloudy, and humid conditions. Typically light precipitation.
Dry Tropical (DT)	Hot, sunny, and dry conditions.
Dry Moderate (DM)	Mild temperatures and dry conditions. Can form when a DP air mass is significantly modified or under periods with zonal flow aloft.
Dry Polar (DP)	Similar to a traditional continental polar (cP) air mass. Often associated with northerly winds. Little to no cloud cover. Adveected in by cold-core anticyclones.

136

137 The NCEP Stage IV data were subset seasonally and by air mass. Statewide and regional values
138 were extracted to calculate the daily average and total precipitation within the respective areas. Daily
139 average precipitation represents the average daily precipitation that fell at each pixel contained
140 within the respective area. The total precipitation is presented in units of millimeter per pixel because
141 it represents the total accumulated precipitation averaged across all pixels contained within each
142 respective area. Averaging total precipitation across the respective area rather than adding
143 precipitation accumulation of each grid cell (i.e. pixel) allowed for the comparison of precipitation
144 accumulations between regions by normalizing differences in area. Thus, the daily average is
145 providing a rate of precipitation at each pixel while the total is providing the total accumulated
146 precipitation per grid cell for the relative temporal subsets in the study period.

147 Maps produced from a Local Indicators of Spatial Association (LISA) [28] analysis facilitated the
148 assessment of statistically significant high and low precipitation clusters within each of the three
149 North Carolina regions independently. The LISA analysis was conducted on each North Carolina
150 region independently to investigate clustering. The goal of the LISA analysis was to identify general
151 patterns as reference for forecasters and identify areas of interest for further research. The LISA
152 analysis used the 16-year integrated daily average precipitation for each of the air mass
153 classifications. In this analysis, a local Moran's I spatial statistic was calculated for each cell based on
154 a queen contiguity spatial neighborhood weight object, and one-sided ($\alpha = 0.05$) hypothesis
155 testing was performed.

156 In a typical global Moran's I approach, the Moran's statistic is structurally similar to a Pearson
157 correlation coefficient where the Moran's statistic compares neighboring grid cell z-scores and, if the
158 grid cells have similar values, the term will be positive (i.e. positive spatial autocorrelation) because
159 both grid cells will tend to be either above the sample mean or below the sample mean. However,
160 this global Moran's I approach only provides information on the general tendency of the dataset to
161 be clustered. Localizing the Moran's I through the LISA approach instead calculates a Moran's I
162 statistic and measure of significance at each grid cell. In the current study, this was done by
163 comparing the weighted z-score at each location with the sample mean, which was bounded by each
164 North Carolina geographic region (i.e. WNC, CNC, ENC). This approach was appropriate due to the
165 distinct geological and anthropogenic differences between the three regions. Calculating significance
166 at each grid cell consisted of a Monte Carlo procedure where actual grid cell values are compared to
167 data values randomly generated and spatially distributed by a permutation procedure. If the
168 observed values exceeded the 95th percentile of the simulated distribution, then it was said to be
169 significant at the 0.05 α value. Through this process, statistically significant positive spatial
170 autocorrelation of high values (illustrated as red colors) and low values (illustrated as blue colors)
171 were identified and plotted. Another important outcome from the LISA analysis was the ability to
172 identify outliers. Those are instances when a high (low) value was located in the vicinity of a low
173 (high) value cluster. This produces statistically significant high-low and low-high spatial outliers;
174 however, because the NCEP Stage IV data is a 4 km gridded product quality controlled at each RFC,
175 these outliers were rare. Nonetheless, it was important to include these spatial outlier measures as it
176 would indicate either unique precipitation conditions or data errors that carried through the quality
177 control procedure.

178 Further, the LISA analysis is not constrained to adjacent pixels. It is possible to assess the effect
179 of using a decayed distance spatial weighting scheme. This allowed us to address the impact of
180 modifying the neighborhood for each grid cell based on distance from the grid cell of interest. After
181 analyzing the impacts of 8 km, 12 km, 16 km, and 20 km spatial weighting schemes, it was found that
182 8 km produced the same results as using the applied queen contiguity neighborhood spatial weight.
183 This is due to the fact that at a 4 km grid cell resolution an 8 km spatial weight would only include
184 those pixels adjacent to the grid cell of interest, the same as the queen contiguity. Additional
185 variations to the neighborhood spatial weight of the Local Moran's statistic had little impact on the
186 overall cluster pattern; however, increased spatial weighting distances (e.g. 12 km, 16 km, and 20 km)
187 unrealistically generalized precipitation patterns and eliminated small scale precipitation clustering
188 characteristics. Specifically, those precipitation clusters analogous with orographic processes were
189 notably lost when neighborhood spatial weights were set too large. It was therefore determined that
190 the queen contiguity neighborhood spatial weight was optimal for the NCRP stage IV 4 km resolution
191 dataset and resolved both homogenous and heterogeneous precipitation events.

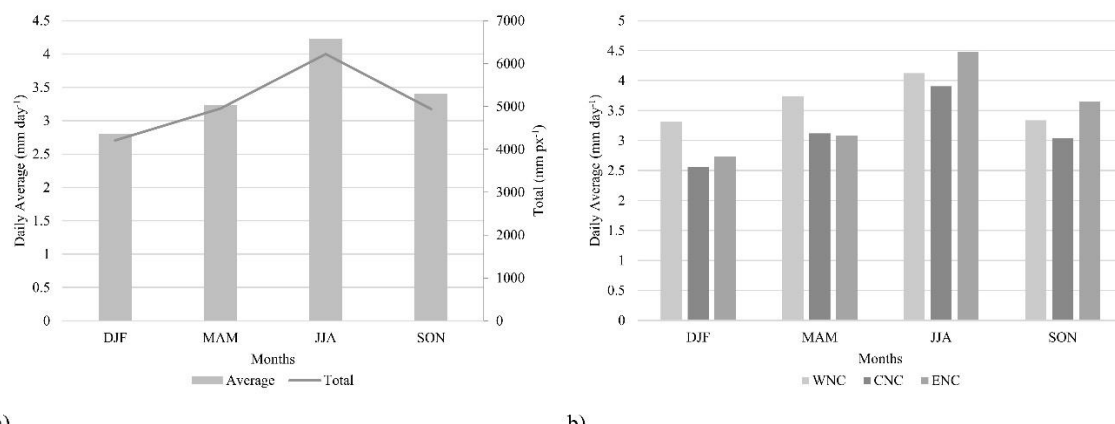
192 3. Results and discussion

193 3.1. General Seasonal Patterns

194 The summer months produced the highest daily average and total rainfall across North Carolina
195 whereas the winter months have the lowest (Figure 2a). This is consistent within all regions of North
196 Carolina (Figure 2b). However, spatial comparisons of daily average precipitation between regions

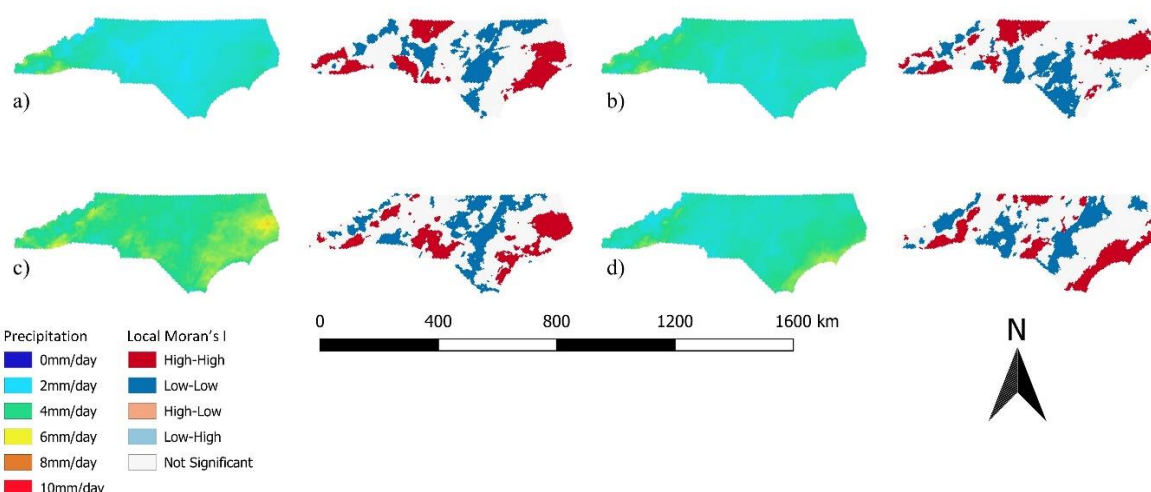
197 shows that there is a seasonal signal to precipitation maximums across regions (Figure 3). WNC
 198 received higher daily average precipitation than CNC and ENC in the winter and spring months,
 199 whereas ENC received higher daily average precipitation during the summer and fall months. Spatial
 200 patterns follow typical characteristic where there tends to be a precipitation maximum on the east
 201 side of the Appalachian Mountains and along the coastal sandhills (Figure 3). However, this signal is
 202 minimized in the winter months (Figure 3a) where precipitation events tend to be driven by
 203 northwest flow events after the passage of mid-latitude cyclones. This leads to conditions where the
 204 southwestern portion of the Appalachian Mountains observed statistically significant clustering of
 205 high daily precipitation amounts. Consistent with Koch and Ray [6], the precipitation maximum over
 206 eastern North Carolina is associated with sea breeze circulations that are further enhanced by distinct
 207 variations in soil composition.

208 Spatial precipitation patterns tend to be less consistent across central North Carolina. In the
 209 winter and spring months, there is clustering of high precipitation values in the northwest portion of
 210 CNC, possibly related to redevelopment of mesoscale convective systems (MCSs) on the east side of
 211 the Appalachian Mountains [5]. In the summer months, this northwest clustering signal is overcome
 212 by a region of high precipitation near the Charlotte metropolitan area. It is possible that this is an area
 213 of precipitation enhancement downwind of the urban city center as noted by studies near similar
 214 metropolitan areas [17,20,21]; however, there is a need for future research detailing the urban
 215 influence on precipitation across North Carolina. The clustering of high precipitation values in the
 216 northern portion of CNC and in the southeastern portion of CNC return in the fall months. This is
 217 likely the return of synoptically driven organized MCS precipitation events propagating eastward
 218 across the state.



219 a) b)
 220 Figure 2. a) Statewide precipitation daily average and total precipitation and b) regional assessment
 221 of daily average precipitation for western North Carolina (WNC), central North Carolina (CNC), and
 222 eastern North Carolina (ENC). Totals are presented as millimeters per pixel (mm px⁻¹) which is
 223 equivalent to millimeters per grid cell.

224



225

226 Figure 3. Daily average precipitation (left) and spatial clustering analysis of precipitation (right) for
 227 DJF (a), MAM (b), JJA (c), and SON (d) over the 2003-2018 study period. Local Moran's I was
 228 calculated within each region individually.

229 3.2. Seasonal and Air Mass Precipitation Patterns

230 It was important to augment the seasonal analysis by focusing on prevailing synoptic-scale air
 231 mass conditions to distinguish between synoptically driven and local-scale thermodynamically
 232 driven precipitation events within each season. Whereas polar air mass conditions tend to be
 233 affiliated with kinetically-driven frontal precipitation, tropical air mass conditions are commonly
 234 used as a proxy for synoptically benign conditions and thermodynamically driven precipitation [20-
 235 22,27]. Also, changes in seasonal air mass frequency may play a role in precipitation distribution and
 236 intensity; therefore, it is important to quantify patterns of both air mass type and air mass frequency
 237 in documenting seasonal precipitation patterns.

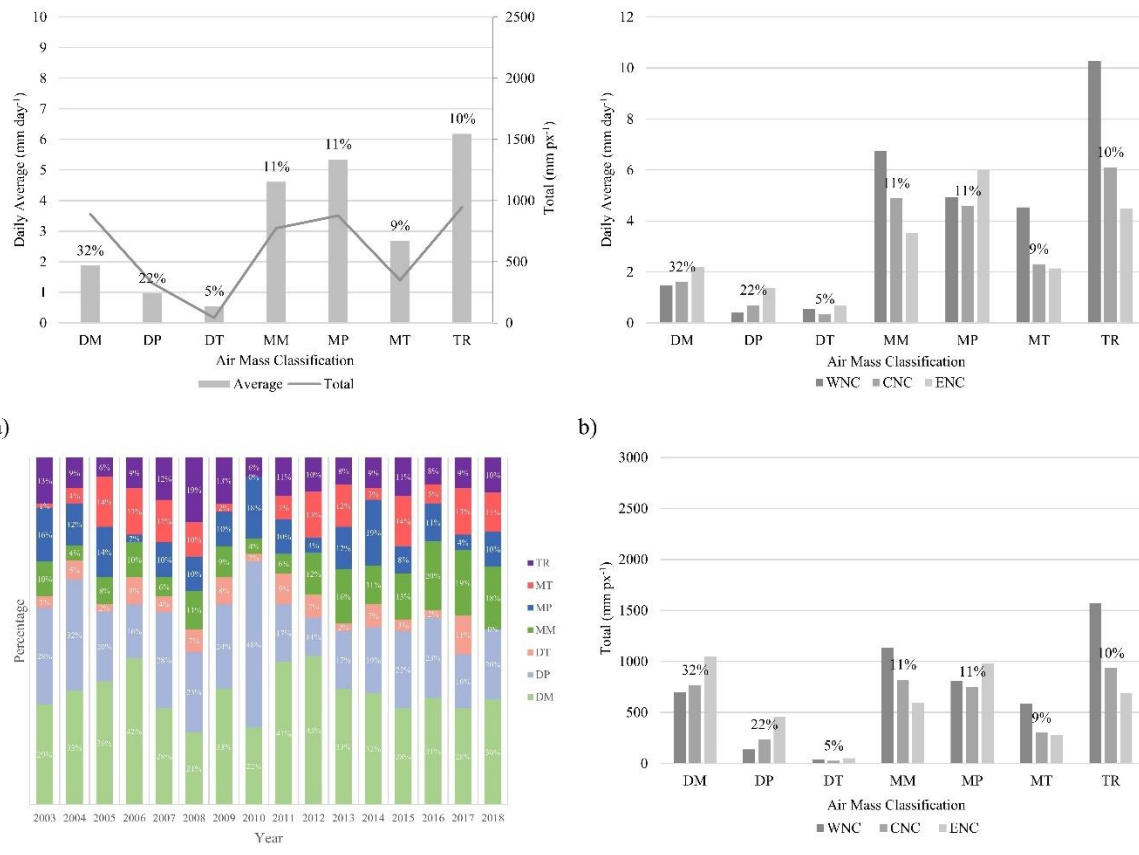
238 3.2.1. Winter

239 Winter months are most often characterized by DM and DP air mass conditions (Figure 4a),
 240 although, while DM and DP dominate the frequency of precipitation and are often associated with
 241 the passage of mid-latitude cyclones, MM and MP conditions make substantial contributions to
 242 wintertime precipitation totals (~40%). Transitional (TR) air mass conditions also make important
 243 contributions to wintertime precipitation. Considering that TR air mass conditions are best described
 244 as a blend of the two transitioning air masses, air mass classifications before and after TR days were
 245 analyzed to identify the most likely conditions occurring under TR days. In the winter, DM air mass
 246 conditions accounted for 35% of days adjacent to TR days, followed by DP (28%), MM (13%), MT
 247 (11%), MP (7%), and DT (6%) conditions. Thus, it is possible that DM and DP contribute more to the
 248 total precipitation, although, TR days may signify unique conditions conducive to high precipitation
 249 amounts due to the transitioning of certain air masses, particularly in WNC where the highest daily
 250 average and total precipitation occur during TR air mass conditions (Figures 4b & 4d). It will be
 251 important for future research to further analyze the air masses undergoing transition in conjunction
 252 with composite circulations to better understand precipitation forcing under TR days.

253 Because MP air mass conditions can result from a DP air mass acquiring additional moisture,
 254 MP air mass conditions are often associated with the passage of mid-latitude cyclones. MM air mass
 255 conditions produce similar conditions to the MP with the exception of having higher temperatures
 256 and higher humidity levels. Furthermore, these MM air mass conditions can form independently to
 257 the south of MP air masses, for example, when a deep mid-latitude cyclone taps into southerly Gulf
 258 moisture. Overall, precipitation totals from DM, DP, MP, and MM air mass conditions make up 68%
 259 of total precipitation; 87% after accounting for the precipitation potentially associated with these air

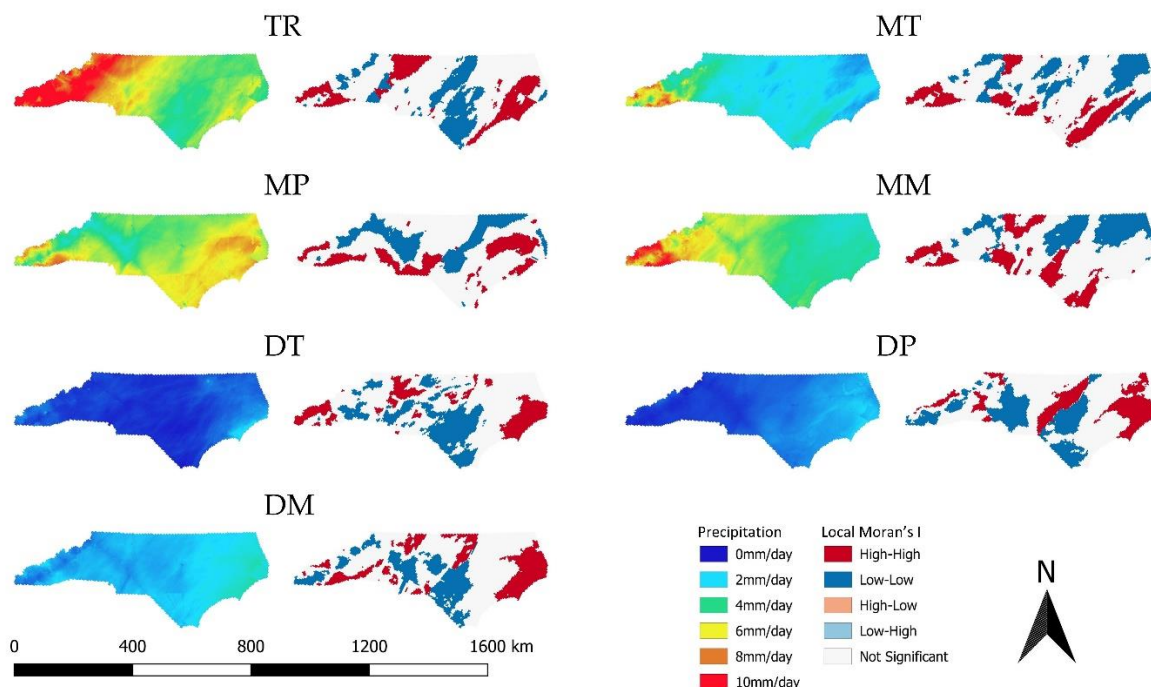
260 mass conditions while undergoing transition during TR days. Regionally, precipitation totals from
 261 DM, DP, MP, and MM—including precipitation during the transition of these air masses—makes up
 262 82%, 87%, and 89% for WNC, CNC, and ENC, respectively. This is consistent with Nieto-Ferreira et
 263 al. [3] who found that 70%–80% of total precipitation across North Carolina is associated with the
 264 passage of a mid-latitude cyclone, with an increasing gradient from WNC to ENC. Interestingly, the
 265 frequency of MM air mass conditions steadily increased from 2010–2018 (Figure 4c). This tends to be
 266 at the expense of DP and MP air mass conditions, suggesting that there has been a gradual shift to
 267 warmer and more humid air mass conditions during the tail-end of the study period (Figure 4c);
 268 however, a longer period of record is required to determine if this trend is a significant shift in
 269 regional conditions or a regional response to other factors, such as teleconnections.

270 Spatial precipitation variations support the above assessment where the highest precipitation
 271 totals and significant clustering of high precipitation amounts occur in the southwest portion and
 272 across the southern portion of the study domain under MM conditions (Figure 5). Precipitation totals
 273 tend to be most homogenous during DT, DP, and DM air mass conditions where there is a gradual
 274 west-to-east increasing gradient in precipitation across North Carolina. Furthermore, areas with
 275 significant clustering of high precipitation amounts under dry air mass conditions tend to cluster
 276 across the northern portion of the study domain suggesting that these events originate poleward of
 277 the study domain. Highest rain amounts in ENC are associated with MP events. In addition,
 278 enhanced clustering of high precipitation amounts in the southern portion of the domain during MP
 279 and MM supports the possibility that these air mass conditions result from the northward advection
 280 of Gulf moisture during the passage of mid-latitude cyclones.



281 c) d)

282 Figure 4. a) DJF statewide daily average precipitation and total precipitation for each SSC air mass
 283 classification; b) daily average precipitation for each North Carolina region; c) frequency of each SSC
 284 air mass classification over the study period; d) total precipitation for each North Carolina region.
 285 Percentages indicate the fraction of air mass classification for each season (a, b, d) or year (c). Totals
 286 are presented as millimeters per pixel (mm px⁻¹) which is equivalent to millimeters per grid cell.



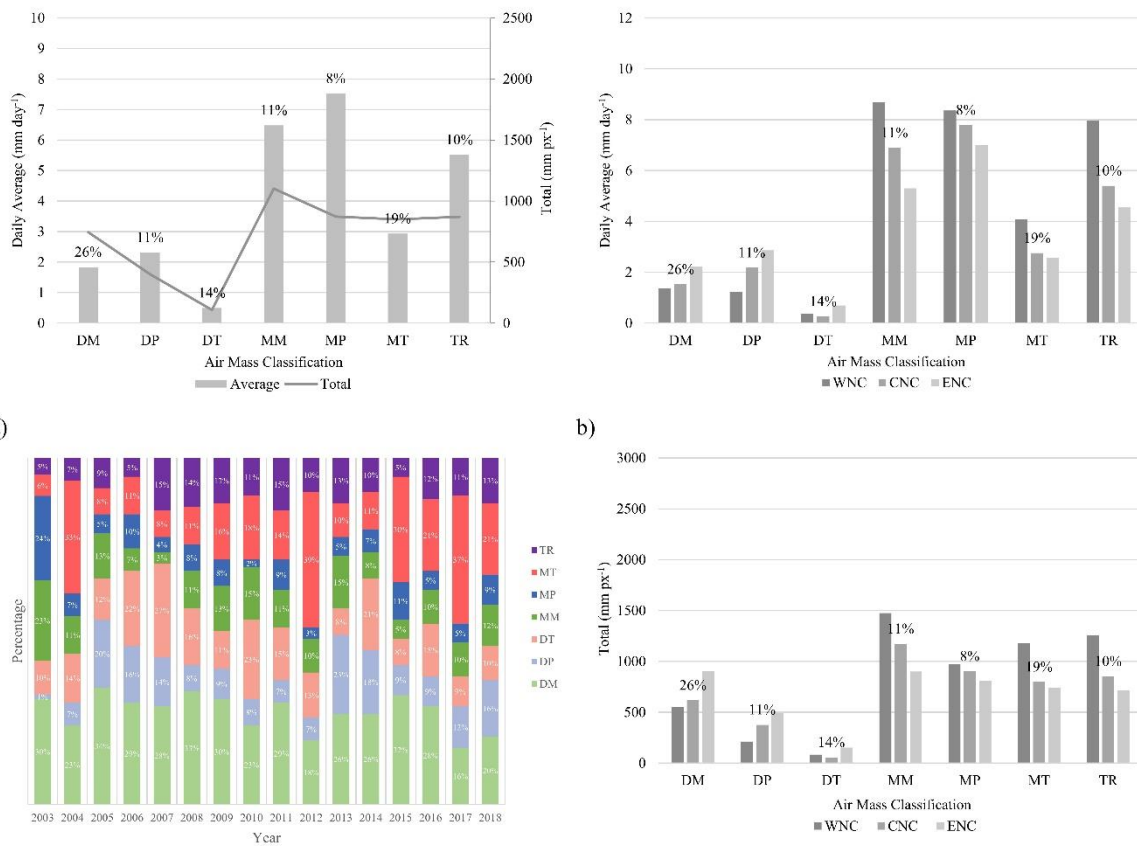
287

288 Figure 5. DJF daily average precipitation (left) and spatial clustering analysis of precipitation (right)
 289 for each SSC air mass classification.

290 3.2.2. Spring

291 The springtime distribution of air mass conditions is similar to the winter; however, there is a
 292 decrease in the frequency of DM and DP air mass days and an increase in the number of MT and DT
 293 days (Figure 6). Similar to winter months, TR days are most often associated with DM air mass
 294 conditions (30%); however, there is a notable increase in the number of TR days associated with DT
 295 (18%) and MT (17%) days at the expense of DP (19%) and MP (4%) days. This is consistent with the
 296 expected transition from a strong synoptic winter regime toward the relatively weak synoptic
 297 summer regime [3]. There is a notable shift to more intense precipitation conditions across all three
 298 regions (Figure 6b). Thus, there is an affiliated increased risk for hazardous hydrometeorological
 299 events due to the shift to air mass conditions conducive to high intensity precipitation events.

300 While dry air mass conditions maintain significant clustering of high precipitation toward the
 301 northern portion of North Carolina, moist air mass conditions no longer have a southern tendency in
 302 the clustering of high precipitation amounts (Figure 7). MT springtime days are characterized by a
 303 northern distribution of high precipitation clustering; however, the clusters are more localized and
 304 sporadic for all moist air mass regimes suggesting a shift toward thermodynamically driven
 305 precipitation events and enhanced connectivity between land-cover conditions and precipitation.
 306 This is an important consideration because it also appears from visual inspection that there is an
 307 increased percentage of MT days during spring months (Figure 6c). This comes at the expense of
 308 fewer DM, DP, and DT days suggesting a shift to more humid springtime air mass conditions
 309 conducive to thermodynamically driven precipitation events.

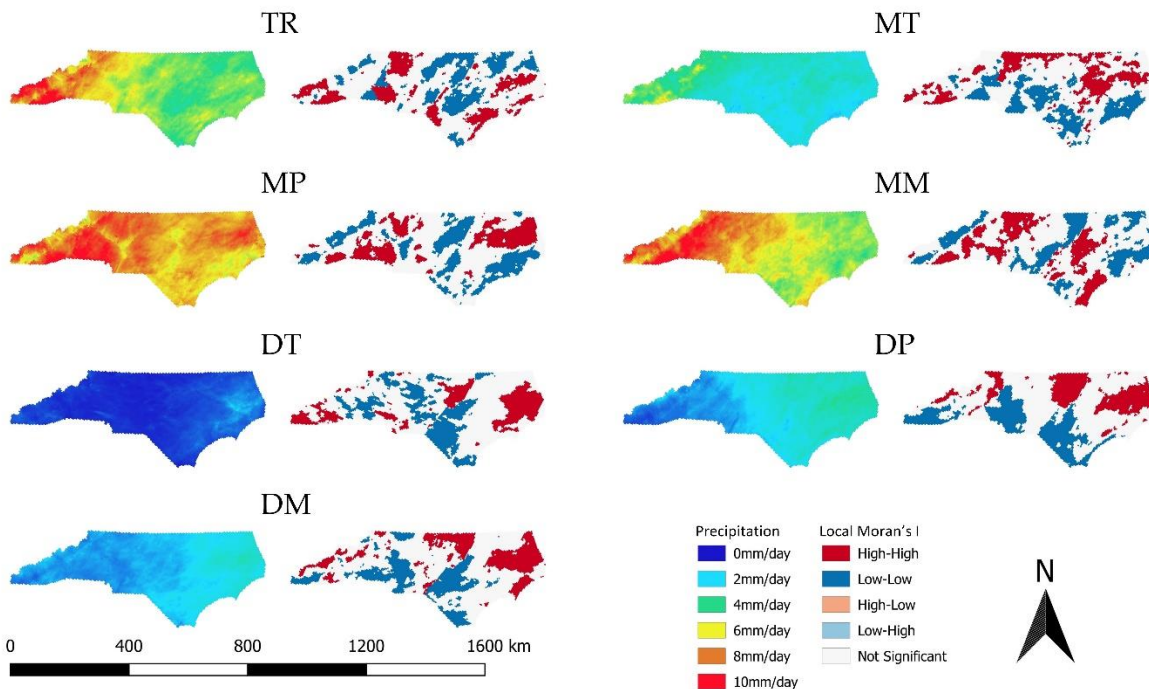


310

c)

311

Figure 6. Same as figure 4 but for MAM.



312

313

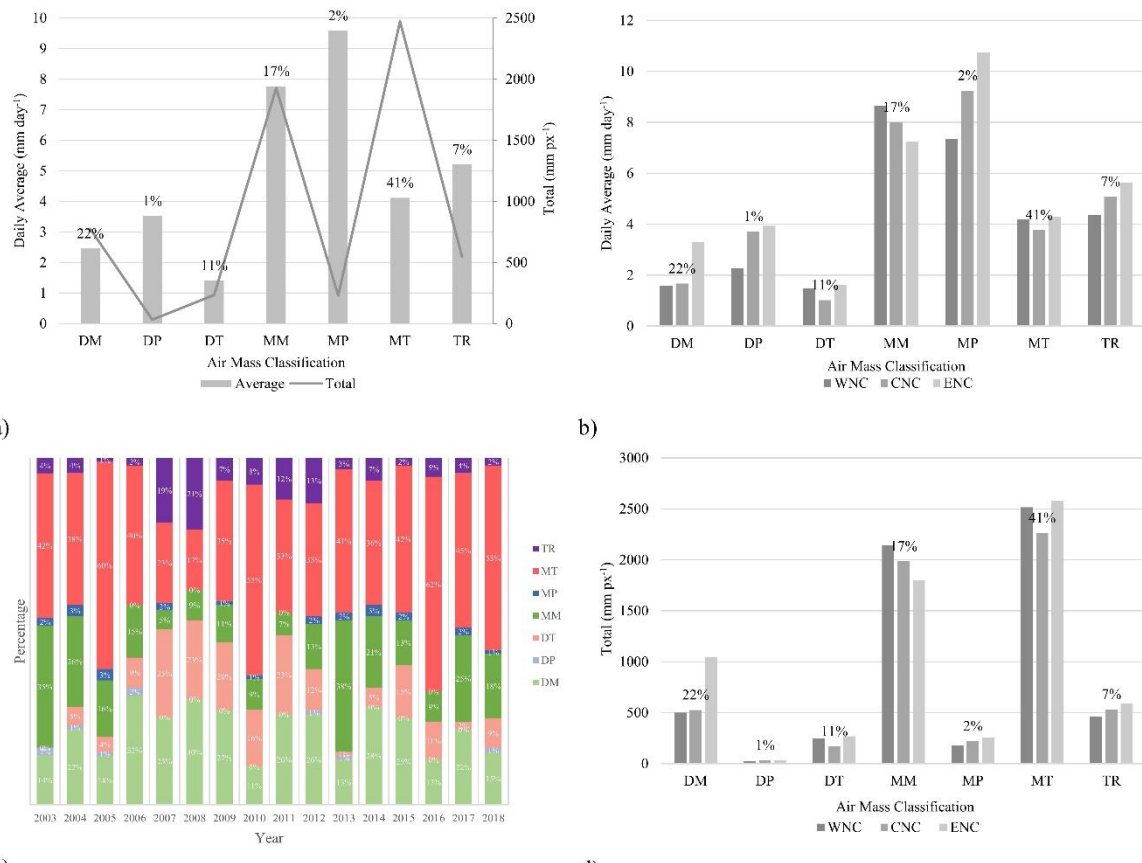
Figure 7. Same as Figure 5 but for MAM

314

3.2.3. Summer

315 There is an abrupt increase in daily average rainfall in the summer months and a shift to a higher
 316 frequency of synoptically benign MT days (Figure 8). These MT days make up 41% of the daily
 317 summertime air mass regimes, followed by DM, MM, DT, TR, MP, and DP; however, DM days
 318 neighbor TR days 30% of the time, with MT days accounting for 29%. DT days combine for 21% of
 319 days adjacent to TR days followed by MM conditions (16%). DP and MP combine to contribute only
 320 4% of days adjacent to TR days. While there are a limited number of days subject to MP air mass
 321 conditions (2%), these air mass conditions are conducive to intense precipitation events (Figure 8b &
 322 Figure 9). Also notable was the substantial contributions to total precipitation from MM air mass
 323 conditions. While MM days make up only 17% of summertime days, they contribute the second
 324 largest amount to total precipitation (31%, Figure 8b). Unlike the winter and spring, there was no
 325 clear visual shift in the frequency of air mass conditions over the period of the study (Figure 8c).

326 The spatial patterns of summer precipitation exhibit a heterogeneous distribution of
 327 precipitation across North Carolina (Figure 9). There maintains significant clustering in the coastal
 328 plains, but the previously strong clustering in the southwest Appalachian Mountains weakened, and
 329 precipitation appears to be heavily impacted by local-scale orographic processes in western North
 330 Carolina. Under the majority of summertime air mass conditions, there is significant clustering near
 331 the urbanized Triad (i.e. Winston-Salem, Greensboro, High Point) region in CNC. It has been
 332 documented that population growth and urbanization across the CNC have contributed to increasing
 333 trends in urban heat island signatures [19]. As observed around other metropolitan areas [17,20,21],
 334 it is possible that the pockets of significant precipitation clustering in CNC are associated with local-
 335 scale thermodynamic forcing and land cover boundaries, which prompts a need for future research
 336 to assess the influence of land cover on precipitation across North Carolina.

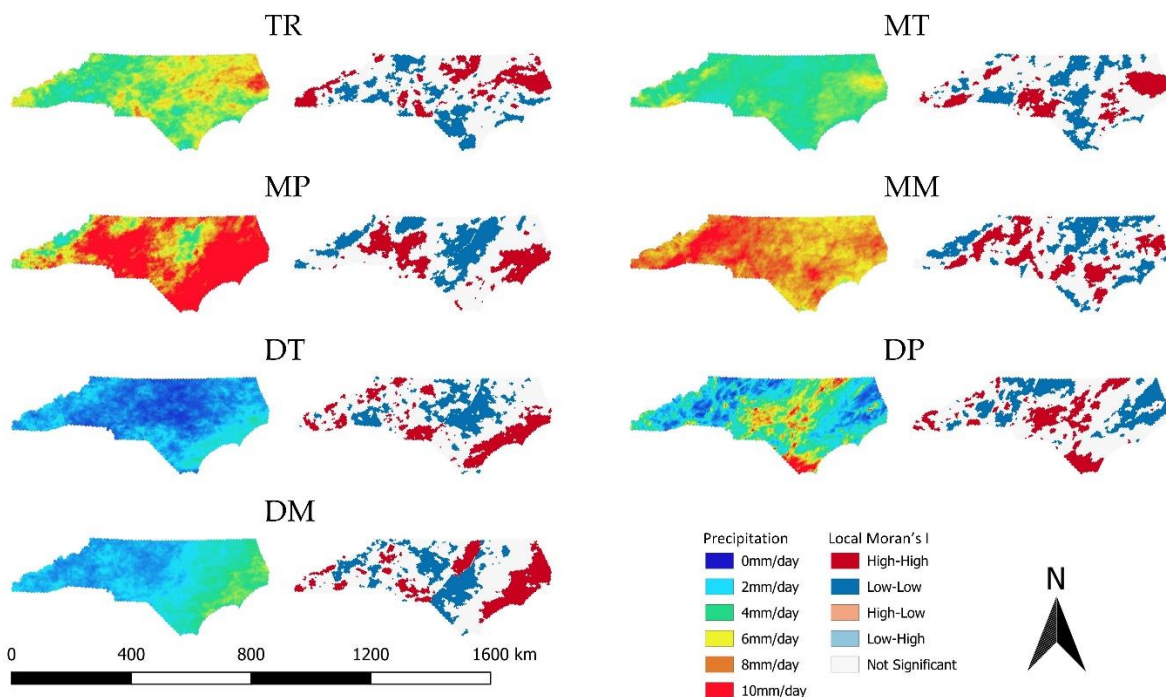


337

c)

338

Figure 8. Same as figure 4 but for JJA.



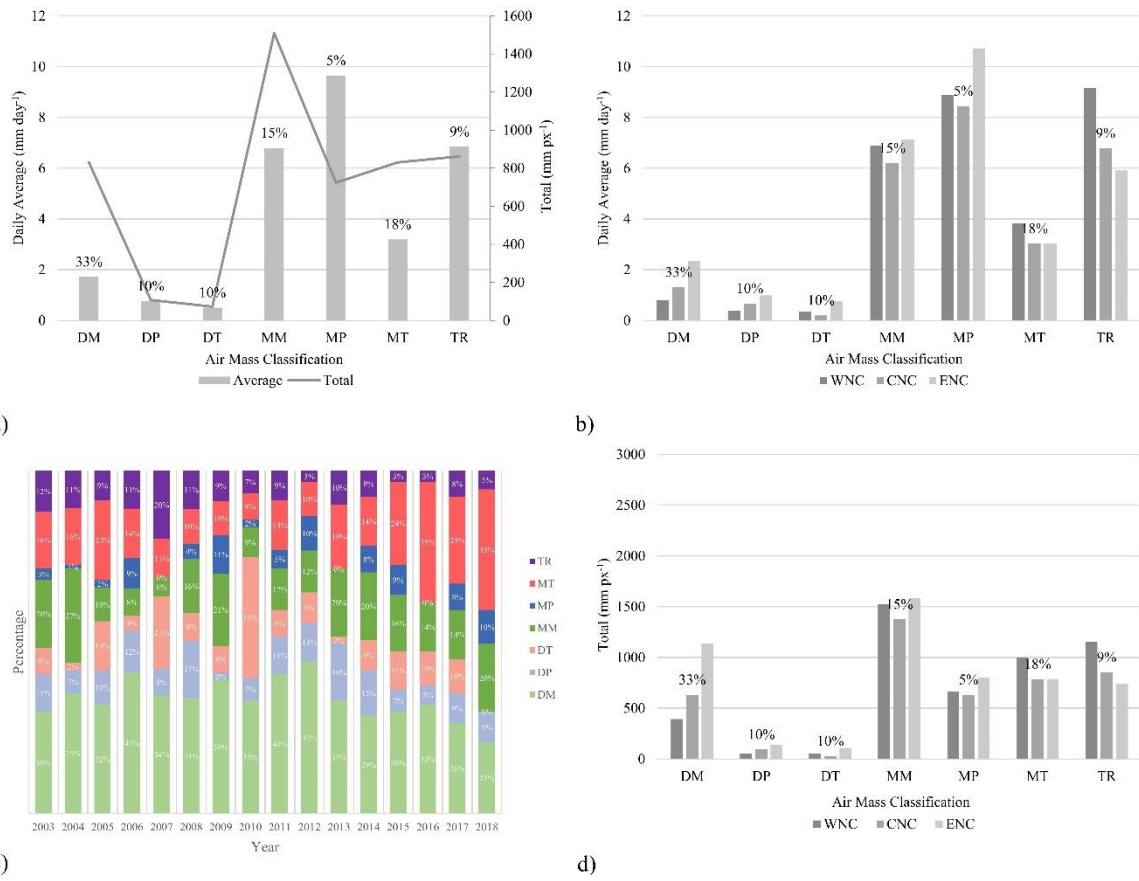
339

340 Figure 9. Same as Figure 5 but for JJA

341 3.2.4. Fall

342 Fall is indicative of a shift away from synoptically benign conditions in the summer to the typical
 343 strong synoptic scale forcing in the winter (Figure 10). There is a shift from MT air mass conditions
 344 to a higher frequency of MP and DM air mass conditions. While the signal in statewide daily average
 345 and total precipitation is similar to the spring months, fall is unique in that daily average precipitation
 346 in ENC during MM and MP days is greater than WNC (Figure 10b). This is likely related to an
 347 increase in mid-latitude cyclone activity coinciding with antecedent summertime patterns favorable
 348 for moisture advection. Fall months exhibited a large decrease in the percent of DT days (9%) adjacent
 349 to TR days; a value closer to what was found in wintertime DT days (6%). As in all seasons, DM days
 350 (36%) is most often adjacent to TR days, followed by DP (21%), MM (16%), MT (14%), and MP (4%)
 351 days.

352 Similar to the spring months, there is a notable increase in the percentage of days under MT
 353 tropical air mass conditions from 2010-2018 (Figure 10c). This is an important outcome because it
 354 appears the transitional and winter month air mass conditions are becoming warmer and more
 355 humid over the period of the study. A spatial pattern that distinguishes the fall from the spring
 356 months is an area of high precipitation amounts clustered over the southeast portions of the domain
 357 (Figure 11). Under MT conditions, this is most likely associated with the passage of tropical cyclones,
 358 whereas the southeastern clustering during DT and DM are likely associated with the passage of mid-
 359 latitude cyclones, sea breeze circulations, or a combination of both.

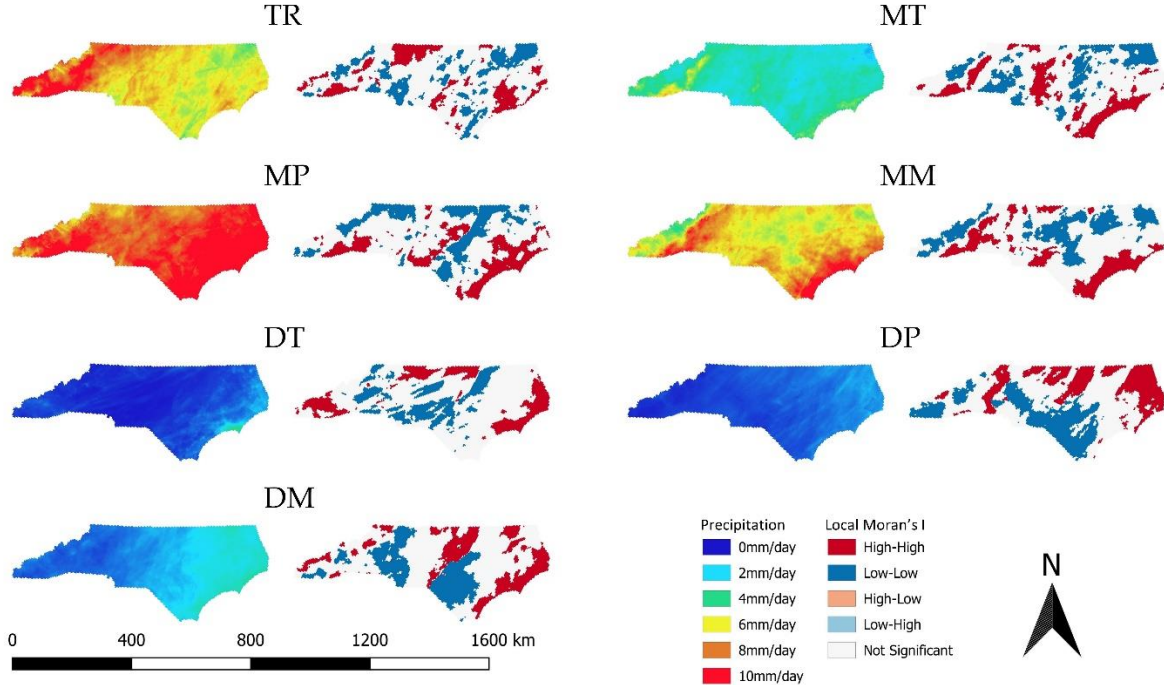


360

c)

361

Figure 10. Same as figure 4 but for SON.



362

363

Figure 11. Same as Figure 5 but for SON

364

4. Conclusions

365 The current study used 16 years (2003-2018) of the National Center of Environmental Prediction
366 (NCEP) Stage IV precipitation dataset to characterize the impact of air mass conditions on seasonal
367 precipitation patterns in North Carolina. Results from the current study aid forecasting and
368 mitigation of hydrometeorological hazards in North Carolina by documenting the spatial and
369 temporal patterns of precipitation magnitude in the context of prevailing air mass conditions. It was
370 found that winter is dominated by dry moderate (DM) and dry polar (DP) air mass conditions
371 indicative of synoptically-driven precipitation events. Spatial clustering confirms this conclusion
372 where there tends to be clustering of high precipitation amounts on the east side of the Appalachian
373 Mountains and along the Coastal Plains. With an increased number of moist tropical (MT) and dry
374 tropical (DT) days, springtime illustrates a shift from synoptically-driven precipitation events to
375 weak synoptic forcing conditions, leading to a greater influence of topography and
376 thermodynamically driven events. North Carolina experiences more heterogeneous and higher daily
377 average precipitation amounts in the spring than winter months. Summertime precipitation is more
378 heterogeneous due to prevailing MT air mass conditions indicating a tendency toward localized and
379 more intense thermodynamically driven precipitation events. Furthermore, it was discovered that
380 while moist moderate (MM) and moist polar (MP) air mass conditions were less frequent, they
381 exhibited the highest daily average rainfall rates suggesting that MM and MP air mass conditions are
382 conducive to hazardous hydrometeorological events. While high humidity levels in the fall maintain
383 high daily precipitation totals under moist air mass conditions, there is a return in wintertime
384 characteristics as the percentage of DP and DM days have a notable increase. In addition, the
385 heterogeneous summertime precipitation spatial distribution begins to give way to spatial patterns
386 more similar to the winter months.

387 With the patterns identified in the current study, future research should use the spatial
388 clustering outcomes to identify and examine areas where small-scale clustering of high precipitation
389 amounts coincides with local-scale variations in land cover conditions. In addition, there is a need to
390 understand the magnitude of correlations between air mass conditions and large-scale
391 teleconnections. This analysis should include an investigation of composite circulations associated
392 with each air mass to characterize the synoptic and mesoscale processes associated with each air mass
393 classification in the Southeast United States. A notable result of this study was that winter, spring,
394 and fall months exhibit a shift to warmer and more humid MM and MT air mass conditions over the
395 2003-2018 study period. This shift could lead to more thermodynamically driven and more intense
396 precipitation events, especially during the spring and fall transitional seasons; however, a longer
397 period of record in addition to air mass trend analyses across North Carolina are needed to assess the
398 significance of these tendencies.

399 **Funding:** This research received no external funding

400 **Conflicts of Interest:** The authors declare no conflict of interest

401 **Author Contributions:** Conceptualization, Christopher Zarzar and Jamie Dyer; Data curation, Christopher
402 Zarzar and Jamie Dyer; Formal analysis, Christopher Zarzar; Investigation, Christopher Zarzar; Methodology,
403 Christopher Zarzar and Jamie Dyer; Project administration, Christopher Zarzar; Resources, Christopher Zarzar;
404 Writing – original draft, Christopher Zarzar; Writing – review & editing, Jamie Dyer.

405 **References**

- 406 1. Seto, K.C.; Shepherd, J.M. Global urban land-use trends and climate impacts. *Curr. Opin. Environ. Sustain.* **2009**, *1*, 89–95.
- 407 2. Bureau, U.C. Fastest-Growing Cities Primarily in the South and West Available online: <https://www.census.gov/newsroom/press-releases/2019/subcounty-population-estimates.html> (accessed on Aug 14, 2019).
- 408 3. Ferreira, R.N.; Hall, L.; Rickenbach, T.M. A climatology of the structure, evolution, and propagation of
409 midlatitude cyclones in the southeast united states. *J. Clim.* **2013**, *26*, 8406–8421.
- 410 4. Shepherd, J.M.; Grundstein, A.; Mote, T.L. Quantifying the contribution of tropical cyclones to extreme

- 414 rainfall along the coastal southeastern United States. *Geophys. Res. Lett.* **2007**, *34*, 1–5.
- 415 5. Parker, M.D.; Ahijevych, D.A. Convective Episodes in the East-Central United States. *Mon. Weather Rev.*
416 *2007*, *135*, 3707–3727.
- 417 6. Koch, S.E.; Ray, C. a. Mesoanalysis of Summertime Convergence Zones in Central and Eastern North
418 Carolina. *Weather Forecast.* **1997**, *12*, 56–77.
- 419 7. Dyer, J. Analysis of a Warm-Season Surface-Influenced Mesoscale Convective Boundary in Northwest
420 Mississippi. *J. Hydrometeorol.* **2011**, *12*, 1007–1023.
- 421 8. Boyles, R.P.; Raman, S. Analysis of climate trends in North Carolina (1949–1998). *Environ. Int.* **2003**, *29*,
422 263–275.
- 423 9. Sayemuzzaman, M.; Jha, M.K. Seasonal and annual precipitation time series trend analysis in North
424 Carolina, United States. *Atmos. Res.* **2014**, *137*, 183–194.
- 425 10. Shepherd, J.M.; Burian, S.J. Detection of Urban-Induced Rainfall Anomalies in a Major Coastal City.
Earth Interact. **2003**, *7*, 1–17.
- 426 11. Krajewski, W.F.; Ciach, G.J.; Habib, E. An analysis of small-scale rainfall variability in different climatic
427 regimes. *Hydrol. Sci. J.* **2003**, *48*, 151–162.
- 428 12. Parker, M.D.; Knievel, J.C. Do meteorologists suppress-thunderstorms? Radar-derived statistics and the
429 behavior of moist convection. *Bull. Am. Meteorol. Soc.* **2005**, *86*, 341–358.
- 430 13. Dyer, J.L.; Garza, R.C. A Comparison of Precipitation Estimation Techniques over Lake Okeechobee,
431 Florida. *Weather Forecast.* **2004**, *19*, 1029–1043.
- 432 14. Dyer, J. Evaluation of Surface and Radar-Estimated Precipitation Data Sources Over the Lower
433 Mississippi River Alluvial Plain. *Phys. Geogr.* **2009**, *30*, 430–452.
- 434 15. Stevenson, S.N.; Schumacher, R.S.; Stevenson, S.N.; Schumacher, R.S. A 10-Year Survey of Extreme
435 Rainfall Events in the Central and Eastern United States Using Gridded Multisensor Precipitation
436 Analyses. *Mon. Weather Rev.* **2014**, *142*, 3147–3162.
- 437 16. Moore, B.J.; Mahoney, K.M.; Sukovich, E.M.; Cifelli, R.; Hamill, T.M.; Moore, B.J.; Mahoney, K.M.;
438 Sukovich, E.M.; Cifelli, R.; Hamill, T.M. Climatology and Environmental Characteristics of Extreme
439 Precipitation Events in the Southeastern United States. *Mon. Weather Rev.* **2015**, *143*, 718–741.
- 440 17. Dixon, P.G.; Mote, T.L. Patterns and Causes of Atlanta's Urban Heat Island–Initiated Precipitation. *J.*
441 *Appl. Meteorol.* **2003**, *42*, 1273–1284.
- 442 18. Rickenbach, T.M.; Nieto-Ferreira, R.; Zarzar, C.; Nelson, B. A seasonal and diurnal climatology of
443 precipitation organization in the southeastern United States. *Q. J. R. Meteorol. Soc.* **2015**, *141*, 1938–1956.
- 444 19. Doran, E.M.B.; Golden, J.S. Climate & Sustainability Implications of Land Use Alterations in an
445 Urbanizing Region: Raleigh-Durham, North Carolina. *J. Environ. Prot. (Irvine, Calif.)* **2015**, *07*, 1072–1088.
- 446 20. Ashley, W.S.; Bentley, M.L.; Stallins, J.A. Urban-induced thunderstorm modification in the Southeast
447 United States. *Clim. Change* **2012**, *113*, 481–498.
- 448 21. Haberlie, A.M.; Ashley, W.S.; Pingel, T.J. The effect of urbanisation on the climatology of thunderstorm
449 initiation. *Q. J. R. Meteorol. Soc.* **2015**, *141*, 663–675.
- 450 22. Sheridan, S.C. The redevelopment of a weather-type classification scheme for North America. *Int. J.*
451 *Climatol.* **2002**, *22*, 51–68.
- 452 23. Tippett, R. NC Demographic Trends Through 2035 House Select Committee on Strategic Transportation
453 Planning and Long Term Funding Solutions. In Proceedings of the House Select Committee on Strategic
454 Transportation Planning and Long Term Funding Solutions; 2016.
- 455 24. Cooperative Distributed Interactive Atmospheric Catalog System/Earth Observing Laboratory/National

- 457 Center for Atmospheric Research/University Corporation for Atmospheric Research, and C.P.C.C. for
458 E.P.W.S.S.D. of C. NCEP/CPC Four Kilometer Precipitation Set, Gauge and Radar Available online:
459 <https://doi.org/10.5065/D69Z93M3> (accessed on Sep 19, 2019).

460 25. Lin, Y.; Mitchell, K.E. The NCEP stage II/IV hourly precipitation analyses: Development and
461 applications. In Proceedings of the 85th AMS Annual Meeting, American Meteorological Society -
462 Combined Preprints; 2005; pp. 1649–1652.

463 26. Nelson, B.R.; Prat, O.P.; Seo, D.-J.; Habib, E.; Nelson, B.R.; Prat, O.P.; Seo, D.-J.; Habib, E. Assessment
464 and Implications of NCEP Stage IV Quantitative Precipitation Estimates for Product Intercomparisons.
465 *Weather Forecast.* **2016**, *31*, 371–394.

466 27. Mote, T.L.; Lacke, M.C.; Shepherd, J.M. Radar signatures of the urban effect on precipitation distribution:
467 A case study for Atlanta, Georgia. *Geophys. Res. Lett.* **2007**, *34*, 2–5.

468 28. Anselin, L. Local Indicators of Spatial Association—LISA. *Geogr. Anal.* **1995**, *27*, 93–115.

469